RT-Fall: A Real-Time and Contactless Fall Detection System with Commodity WiFi Devices

Hao Wang, *Student Member, IEEE*, Daqing Zhang, *Member, IEEE*,
Yasha Wang, *Member, IEEE*, Junyi Ma, Yuxiang Wang, and Shengjie Li

Abstract—This paper presents the design and implementation of RT-Fall, a real-time, contactless, low-cost yet accurate indoor fall detection system using the commodity WiFi devices. RT-Fall exploits the phase and amplitude of the fine-grained Channel State Information (CSI) accessible in commodity WiFi devices, and for the first time fulfills the goal of segmenting and detecting the falls automatically in real-time, which allows users to perform daily activities naturally and continuously without wearing any devices on the body. This work makes two key technical contributions. First, we find that the CSI phase difference over two antennas is a more sensitive base signal than amplitude for activity recognition, which can enable very reliable segmentation of fall and fall-like activities. Second, we discover the sharp power profile decline pattern of the fall in the time-frequency domain and further exploit the insight for new feature extraction and accurate fall segmentation/detection. Experimental results in four indoor scenarios demonstrate that RT-fall consistently outperforms the state-of-the-art approach WiFall with 14 percent higher sensitivity and 10 percent higher specificity on average.

Index Terms—Fall detection, activity recognition, channel state information (CSI), WiFi, phase difference

1 Introduction

Falls are the leading cause of fatal and nonfatal injuries to elders in the modern society [1]. According to the Centers for Disease Control and Prevention, one out of three adults aged 65 and over falls each year [2]. Falls not only bring a main threat to elders' health, they account for a large part of medical cost as well. For example, in 2,000 falls among older adults cost the U.S. health care system over $19 billion dollars and the number increased to $30 billion dollars in 2010 [2]. Most elderly people are unable to get up by themselves after a fall, studies have shown that the medical outcome of a fall is largely dependent on the response and rescue time [3]. The delay of medical treatment after a fall can increase the mortality risk in some clinical conditions, half of those who experienced an extended period of lying on the floor ($>1h$) died within six months after the incident [4]. In addition to physical injuries and high medical cost, falls also cause psychological damage to elders, which is termed as the fear of falling cycle by the fall researchers [5]. The fear cycle refers to the fact that after a fall, even without injury, elders become so afraid of falling again that they reduce physical activities. This in turn decreases their fitness, mobility and balance, leads to decreased social interactions, reduced life satisfaction and increased depression. This fear cycle then increases the risk of another fall [5].

For elders who live alone and independently, about 50 percent of the falls occur within their own homes [1], thus timely and automatic detection of falls has long been the research goal in the assistive living community. Various techniques ranging from wearable sensor-based, ambient device-based to computer vision based solutions have been proposed and studied [3], [6], [7], [8], [9], [10]. *Wearable sensor-based approaches* were among the first techniques developed for fall detection [11]. Since Lord and Colvin [12] proposed an accelerometer-based approach in 1991, numerous kinds of sensors have been explored for fall detection in the past decades, ranging from gyroscopers [13], barometric pressure sensors [14], RFID [15], to the sensor-rich smart phones [16]. These systems can only work when sensors are worn by the user. However, the always-on-body requirement makes the subject difficult to comply with, especially for the elders at home. *Ambient device-based approaches* try to make use of ambient information caused by falls to detect the risky activity. The ambient information being used includes audio noise [7], floor vibration [3], [6] and infrared sensing data [17]. In these systems, dedicated devices need to be implanted in the environment. However, the other sources of pressure or sound around the subject in the environment account for a large proportion of false alarms. *Computer vision-based approaches* use cameras installed in the monitoring environment to either capture images or video sequences for scene recognition. Although the recent advances in infra-red LED and depth camera like Microsoft Kinect [18], [19], have enlarged its application scope (e.g., independent of illumination of lights and can work even in a dark room), the privacy intrusion, inherent requirement for line of sight and intensive computation for real-time processing are still open issues that need to be addressed in the future [8], [10].

- *H. Wang, D. Zhang, J. Ma, Y. Wang, and S. Li are with the Key Laboratory of High Confidence Software Technologies, Ministry of Education, and School of Electronics Engineering and Computer Science, Peking University, Beijing 100871, China. E-mail: {wanghao, dqzhang}@sei.pku.edu.cn, {majunyi, wyxpku, lishengjie}@pku.edu.cn.*
- *Y. Wang is with the National Engineering Research Center of Software Engineering, Peking University, China. E-mail: wangys@sei.pku.edu.cn.*

Manuscript received 1 Sept. 2015; revised 10 Apr. 2016; accepted 12 Apr. 2016. Date of publication 22 Apr. 2016; date of current version 5 Jan. 2017.
For information on obtaining reprints of this article, please send e-mail to: reprints@ieee.org, and reference the Digital Object Identifier below.
Digital Object Identifier no. 10.1109/TMC.2016.2557795

Due to the limitations of the above-mentioned fall detection solutions, very few fall detection systems have been widely deployed in real home settings so far [20]. In recent years, the rapid development in wireless techniques has stimulated the research in studying the relationship between the wireless signal and human activities. In particular, the recently exposed physical layer Channel State Information (CSI) on commercial WiFi devices reveals multipath channel features at the granularity of OFDM subcarriers [21], which is much finer-grained than the traditional MAC layer RSS (Received Signal Strength). By exploiting the amplitude and phase information of CSI across the OFDM subcarriers and the diversity of CSI information across multi-antennas in MIMO systems, significant progress has been made in applications in motion detection [22], [23], lip language [24] and gesture recognition [25], [26], vital sign monitoring [27], [28], and activity recognition [29], [30]. The rationale behind all these research efforts is that different human activities can cause different signal change patterns, and activities can be recognized in real-time by mapping the observed signal change patterns to different human activities. With this motivation, in this paper, we aim to investigate if real-time and automatic fall detection can be achieved using cheap and widely deployed WiFi devices at home, without requiring the subjects to wear or carry any objects.

As far as we know, Wifall [29] is the first work using WiFi commodity devices to detect fall. However, it makes two assumptions: (1) the subject can only perform four kinds of predefined activities (i.e., walk, sit, stand up, fall). (2) Activities can not be performed continuously. Obviously, both assumptions are not realistic in real home settings. Therefore, in this work, we intend to remove these two assumptions to detect the fall in the real settings, i.e., various daily activities are performed naturally and continuously.

In order to automatically detect falls in real-time with WiFi signals in the real settings, there are several challenges that must be addressed. First, how the fall and other human activities affect the amplitude and phase information of CSI? Are there any specific features in the CSI of WiFi signal streams which can characterize the fall and other human activities? Second, as activities are performed continuously, the boundary of the WiFi signal of subsequent activities is not given. How to automatically and accurately segment the corresponding fall and other activities in the continuously captured WiFi wireless signal streams? Third, as there are numerous daily activities, from the perspective of activity recognition, the problem space is large. Even if the activities are segmented out, differentiating the fall from all the other daily activities is also challenging.

In our previous work [31], we observe that the phase difference over two antennas exhibits interesting characteristics in the presence of fall and other human activities, while the raw amplitude and phase information themselves are not directly usable. Based on this observation, we proposed a transition-based segmentation method leveraging the variance of phase difference over a pair of receiver antennas as a salient feature to automatically segment all the fall and fall-like activities in the continuously captured WiFi wireless signal streams. Then we extracted features from both the amplitude and phase information of CSI to separate the fall from the fall-like activities. Leveraging the previous work, we conduct intensive experiments using commodity WiFi devices to empirically study how the amplitude and phase difference of CSI change in both time and frequency domain in the presence of various human activities. In addition to verifying that the phase difference is a more sensitive base signal than the amplitude of CSI, we also observed that the fall and fall-like activities are ended with a sharp power profile decline in the time-frequency domain. Based on these two insights, we design and implement our real-time and non-intrusive fall detector, called RT-Fall. The fall detection process performed by RT-Fall mainly contains two-phases: First, we use the variance of phase difference as a base signal and design a set of filtering and signal processing techniques to robustly segment the fall and fall-like activities in the continuously captured WiFi wireless signal streams. After singling out the fall and fall-like human activities in the wireless signal stream, we extract a set of new features in both the time and frequency domain based on the two insights to differentiate the real fall from the fall-like activities using Support Vector Machine (SVM).

In summary, the main contributions of this work are as follows:

1) To the best of our knowledge, this is the first work to deal with fall detection problem with commodity WiFi devices in the real settings, i.e., detect the fall in the condition that numerous daily activities are performed naturally and continuously.
2) We are the first to identify the phase difference of CSI as a better base signal than amplitude for activity segmentation and fall detection. By studying the relationship between different human activities and the variance of phase difference, we demonstrate its effectiveness as a base signal to segment the fall and fall-like activities in the continuously captured signal streams.
3) We found the sharp power profile decline pattern of the fall in the time-frequency domain and further exploited the complementary characteristics of falls in the time and frequency domain for accurate fall segmentation/detection.
4) We design and implement the real-time activity segmentation and fall detection system, RT-Fall on commodity WiFi devices, with only one antenna at the transmitter side, and two antennas at the receiver side. Experiment results demonstrate that RT-Fall can segment the falls in the WiFi wireless signal streams with an accuracy of 100 percent and consistently outperform the state-of-the-art fall detector WiFall [29], with 14 percent higher sensitivity and 10 percent higher specificity on average.

The rest of the paper is organized as follows. We first review the related work in Section 2 and then introduce preliminaries in Section 3. In Section 4 we report the empirical study results about the relationship between the WiFi CSI information and the human activities, followed by the RT-Fall framework design. Section 6 presents the system performance evaluation results and then we discuss some unaddressed research issues in Section 7. Finally, we conclude our work in Section 8.

2 Related Work

In this section, we review the related work from two perspectives: research on fall detection and research on WiFi CSI-based activity recognition.

2.1 Related Work on Fall Detection

Fall detection has attracted a lot of attention in assistive living and healthcare community for two decades. A great number of fall detection techniques have been proposed since the early 1990s. Noury et al. [9], Yu [10], Natthapon et al. [20] and Spasova et al. [11] reviewed the principles and approaches used in existing fall detection systems. Roughly, the fall detection systems can be classified into three broad categories: wearable sensor based systems, ambient device based systems and computer vision based systems.

Wearable sensor based fall detection systems were among the first efforts about fall detection. They attempt to detect falls leveraging sensors embedded in wearable objects such as coat, belt and watch. Since Lord and Colvin [12] proposed an accelerometer based approach in 1991, various kinds of sensors have been explored to detect fall in the past decades. The widely used sensors include gyroscopes [13], barometric pressure sensors [14], RFID [15]. These detection systems can only work on the premise that all the devices are worn or carried by the subject during fall. Smart phone based fall detector is one of the promising fall detection systems with great potential due to the popularity of sensor-rich smartphones [16]. While these solutions are appropriate for fall detection in outdoor environment, the always-on-the-body requirements make the subjects difficult to comply with, especially for the elders at home.

The ambient device based fall detection systems intend to detect falls in a non-intrusive way by exploiting the ambient information including audio noise [7], floor vibration [3], [6], infrared sensing data [17] produced by a fall. The rational behind these ambient device based fall detection systems is that different human activities will cause different changes in acoustic noise or floor vibration. These solutions do not require the subject to carry or wear anything, they are non-intrusive and more privacy-preserving than computer vision-based systems. However, dedicated devices need to be installed in the dwelling environment. Moreover, false alarms are often incurred by other sources causing the same effect. For example, an object fall might also cause similar effect in vibration or sound as an elder's fall.

Computer vision based fall detection systems use cameras installed in the monitoring environment to either capture images or video sequences for scene recognition. By using activity classification algorithm, the fall activity is distinguished from other events [8] ,[9] ,[10]. Recent advances in infra-red LED and depth camera like Microsoft Kinect [18], [19], have enlarged its application scope (e.g., independent of illumination of lights and can work even in a dark room). However, there are still a set of open issues to be resolved, such as privacy concern, requirement for line of sight and intensive computation for real-time processing [8] ,[10].

2.2 Related Work on WiFi-Based Activity Recognition

The WiFi signal strength RSS has been exploited for indoor localization for more than a decade [32]. However, only recently research attempts have been made to use WiFi RF signal for gesture and activity recognition [25], [29]. While [25], [33] first explore and use WiFi RF signal to recognize different body or hand gestures, they use dedicated instruments to collect special RF signals, which are not accessible with commodity WiFi devices. With the CSI tractable on commodity WiFi devices [21], FCC [34] studies the relationship between the number of moving people and the variation of CSI and thus achieves device-free crowd counting. Liu et al. [27] and Liu et al. [28] exploit the CSI from commodity NICs to extract the human respiration and heart beat rates in a controlled setting. Kosba et al. [22], Qian et al. [23], Liu et al. [35] and Wunon et al. [36] employ RSS and CSI information respectively to detect the human motion in indoor environment. Sigg et al. [37] use software radio to improve the granularity of RSSI values and consequently improve the accuracy of activity recognition. E-eyes [30] uses CSI amplitude histograms as fingerprints to recognize nine different daily human activities. Moreover, Wang et al. [24] and Melgarejo et al. [26] leverage WiFi devices equipped with directional antennas to recognize lip and gesture language respectively. However, all the above WiFi based activity recognition work only deals with problems to recognize activities from a predefined activity set. Unfortunately, the fall detection problem is far more complex. Specifically, first, the fall should be singled out from various daily activities which can not be predefined or collected for training and testing one by one. In other word, the countless human activities make the fall detection problem space very large. Second, when various daily activities are performed continuously, the boundary of the WiFi signal of subsequent activities is not marked. Identifying the starting and finishing point of interested activities for further training and classification is challenging.

The first work using WiFi commodity devices to detect fall is presented in [29], where it exploits the WiFi CSI information for fall detection. But the work only makes use of the amplitude information of CSI and simplifies the problem, i.e., the subject can only perform four kinds of predefined activities. When the elders live normally in the home environment with various activities naturally and continuously performed, the solution will fail. In our earlier work [31], we attempted to leverage both the amplitude and phase information of CSI from commodity WiFi devices to detect fall in real-time. In particular, we proposed to use the phase difference over two antennas as the salient feature for both activity segmentation and fall detection. Different from our previous work, in this paper, we intensively study the relationship between the amplitude, phase, and phase difference of the CSI information and the human activities, respectively, and find that the phase difference is a more sensitive base signal than amplitude or phase for activity recognition. Further more, we discover the sharp power profile decline pattern of the fall in the time-frequency domain. By leveraging the findings about the phase difference and the power profile decline pattern, we design a set of signal processing techniques to robustly segment the fall

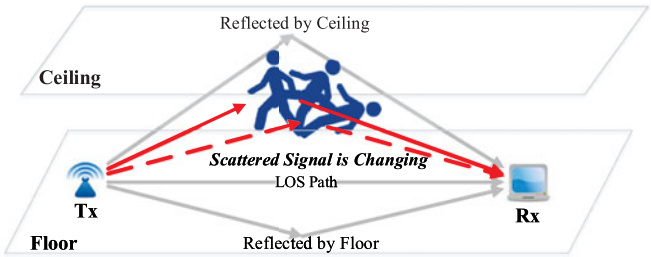

Fig. 1. WiFi signal propagation in indoor environment.

and a few fall-like activities from the other activities. Then with only the fall and fall-like activities separated, we further extract effective features from the amplitude and phase difference of CSI, to distinguish the real fall from other fall-like activities, making the real-time fall detection leveraging the WiFi RF signal streams feasible in real home setting.

3 Preliminaries

In this section, we first introduce the concept of Channel State Information (CSI) in commodity WiFi devices, then we specify the fall activity types targeted in this work.

3.1 Channel State Information in IEEE 802.11n/ac

In a typical indoor environment, as illustrated in Fig. 1, WiFi signals propagate through the physical space via multiple paths such as ceiling, floor, wall and furniture. As the physical space constrains the propagation of wireless signals, the received signals in turn contain information that characterizes the environment they pass through. If a person presents in the environment, additional signal paths are introduced by the scattering of human body. Then, the received signals also convey information that characterizes the effects of human presence in the environment. If we consider the physical space (including ambient objects and human) as a wireless Channel, the Channel State Information depicts the effects when the wireless signals pass through this wireless Channel. In frequency domain, the channel can be modeled as $Y = HX + N$, where Y and X are the received and the transmitted signal vectors respectively, N denotes the channel noise vector and H is the channel matrix. The channel matrix H is presented in the format of Channel State Information. Specifically, current WiFi standards (e.g., IEEE 802.11n/ac) use orthogonal frequency division modulation (OFDM) in their physical layer. OFDM splits its spectrum band (20 MHz) into multiple (56) frequency sub-bands, called subcarriers, and sends the digital bits through these subcarriers in parallel. CSI reveals a set of channel measurements depicting the amplitude and phase of every OFDM subcarrier. CSI of a single subcarrier is in the following mathematical format: $h = |h|e^{j\angle\theta}$, where $|h|$ and θ are the amplitude and phase, respectively.

If there is no one or no motion in the environment, the channel is relative stable. However, as shown in red lines in Fig. 1, along with the motion of a person, the scattered signals are changing, which results in obvious channel distortion, involving both amplitude attenuation and phase shift. *Human activity can be recognized by mapping different channel distortion patterns to corresponding human activities.*

3.2 Fall Activity Types Targeted

There are many ways in which an elder can fall, and in this work we aim to detect falls occurred in situations with respect to two transition activities: 1): standing-fall refers to the situation that the fall occurs when an elder transfers out of a bed or chair, e.g., the elder may just stand up from the chair and falls down; 2): walking-fall refers to situation that the fall occurs while an elder is walking. According to a study by SignalQuest on falls for the elderly, 24 percent of falls occurred in the first case and 39 percent occurred in the second [38]. Hence, we aim for 63 percent of the fall situations in this work and plan to address the other fall types which occur while ascending or descending stairs or engaging in outdoor activities, in future work.

4 Empirical Study

In this Section, we conduct intensive experiments using commodity WiFi devices to empirically study how the amplitude and phase information of CSI across the OFDM subcarriers and multi-antennas change in the presence of different human activities at indoor environment.

4.1 Human Activities and Amplitude of CSI

In this part, we explore the relationship between human activities and the amplitude information of CSI. We first present how the amplitude varies across different subcarriers and different streams respectively, and then we show how the amplitude changes in the presence of different human activities in Line-Of-Sight (LOS) and Non-Line-Of-Sight (NLOS) conditions.

4.1.1 Amplitude Across Different Subcarriers and Streams

As we only use one transmitter antenna and two receiver antennas, CSI information we collected is further divided into two wireless streams and thirty subcarriers in each stream. In this study, we conduct experiments to see how the amplitude varies across different subcarriers and different streams respectively. We have the same observation as [29] that human activities affect different streams independently whereas affect different subcarriers in a similar way. Furthermore, subcarriers among adjacent frequencies share more similarities than those with larger frequency gap. Based on these observations, we can average CSI samples of adjacent successive subcarriers into one signal value to achieve trade-off between computational complexity and functionality. In the rest of this work, we will only show figures with one subcarrier in one stream.

4.1.2 Impact of Different Human Activities

We roughly divide human daily activities into two categories: immobile and motion activities.

Impact of immobile human activities. Immobile activities, such as sitting, lying, and standing, intuitively result in relatively stable signal change patterns as they only involve tiny changes in human bodies (e.g., chest movement caused by respiration, tiny body movement unconsciously). Through extensive experiments, the results roughly fit the intuition. Figs. 2a, 2c show the amplitude variance of three

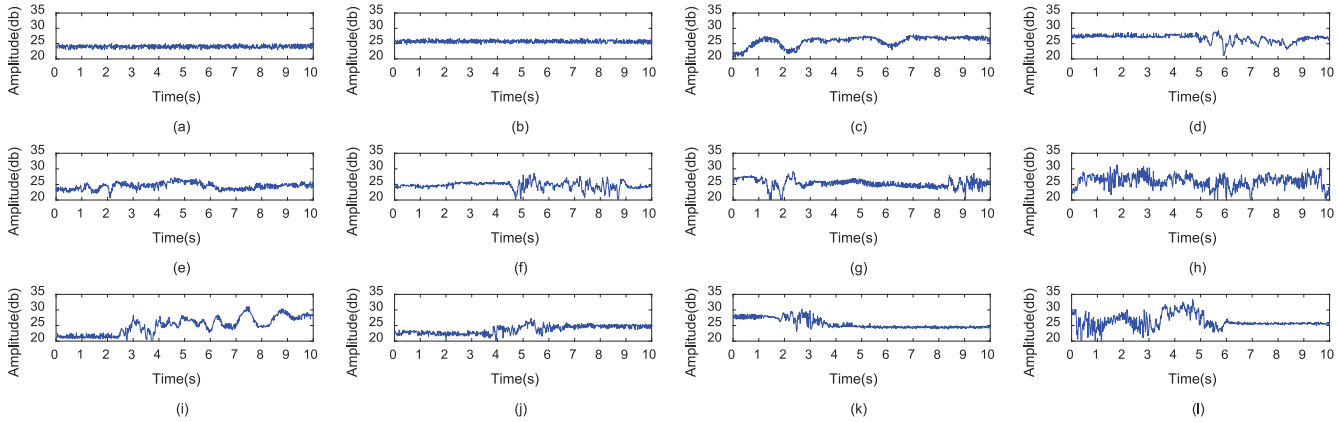

Fig. 2. CSI amplitude of human motion activities: (a) Sitting, (b) Lying, (c) Standing, (d) Lie down, (e) Upper body activities, (f) Pickup, (g) Squat, (h) Walking, (i) Stand up, (j) Sit down, (k) Standing-Fall, and (l) Walking-Fall.

immobile activities, respectively. Interestingly, we have an observation which was not mentioned in previous work that the signal variance of the standing posture seems more notable than that of other immobile activities like sitting and lying. We also note that the amplitude variance of standing reduces when the subject stands farther away from LOS path. Hence, we doubt whether the amplitude can reliably distinguish between the standing posture and other immobile activities. This inspires us to conduct a comprehensive analysis on the impact of LOS/NLOS condition before we can give the answer to this question.

Impact of human motion activities. Compared to immobile activities which result in relatively stable signal changes, motion activities, such as walking, lying down, sitting down and fall, exhibit obvious signal variance as illustrated in Figs. 2d, 2l. To differentiate the fall from other activities, we tried to find some unique features of the fall at first. Unfortunately, neither the variance of the amplitude nor the profile of the amplitude shows clear patterns to make the fall distinguishable from other activities. Therefore, the amplitude can only tell whether the human subject is conducting motion activities or not.

4.1.3 Activities in LOS and NLOS Conditions

As daily activities can occur in different locations in the indoor environment, we conduct activities in both LOS and NLOS conditions to see their impact. As illustrated in Fig. 3, the amplitude variance caused by human activities becomes weaker from LOS to NLOS conditions. This is expected because the signal propagation suffers from path loss [39]. For example, as shown in red lines in Fig. 1, along with the motion of human body, the scattered paths from human body keep changing. With the distance between human body and LOS path increasing, those scattered power decreases rapidly until they become too weak to be distinguished from the environment noise. Then we come up with the following questions: *how far away will the CSI amplitude of the standing posture become indistinguishable from that of other immobile activities? And how far away will this base signal of motion activities become indistinguishable from that of immobile activities?*

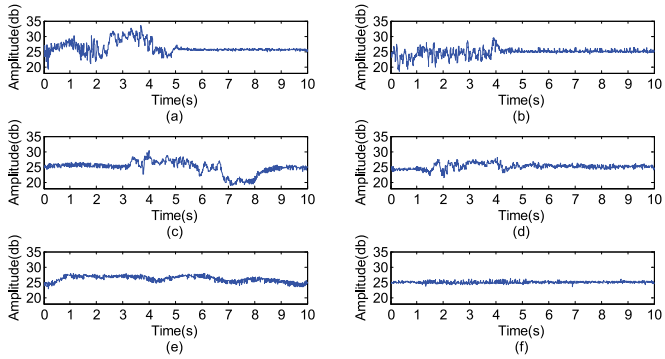

Fig. 3. CSI amplitude of activities in LOS and NLOS conditions: (a) LOS Walking-Fall, (b) NLOS Walking-Fall, (c) LOS Sit down, (d) NLOS Sit down, (e) LOS Standing, and (f) NLOS Standing.

We conduct extensive experiments in different rooms of different sizes, finding that the exact results vary slightly with respect to room settings and layouts. Using the settings we adopt, the answer to the first question is around 2 m in a clear environment, and it drops to less than 1.5 m with a 1 m high wooden desk and an LCD desktop screen on it as an obstacle between the LOS and human. Considering the symmetry of both sides from LOS path, we find that the coverage area is not enough for common rooms. Hence, we conclude that *the ability of the CSI amplitude to distinguish the standing posture from other immobile activities is quite limited and unreliable* in ordinary indoor living environments. The answer to the second question is 5 m without obstacles from LOS path and it drops to 4 m with the same wooden obstacle. Considering the symmetry of both sides from LOS path, the coverage area, even with 4 m, is big enough for a common living room. Hence, *the ability of the CSI amplitude to distinguish the motion activities from immobile ones is enough and reliable* in common living rooms.

4.1.4 Fall in Different Scenarios

We then focus on falls, i.e., standing-fall and walking-fall, occurred in different scenarios, including LOS and NLOS. As illustrated in Fig. 4, the amplitude variance shows a clear transition from a fluctuated state to a stable one among all falls. This is expected because the fall often ends up with an immobile posture (e.g., lying on the floor/sofa) which results in a relatively stable signal change pattern. It seems that we could use the transition as a feature for real time activity segmentation. *Unfortunately, as numerous human daily activities can end up with certain kind of immobile activities,*

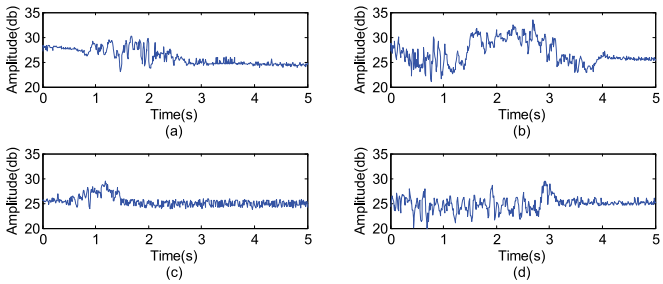

Fig. 4. Fall in different Scenarios: (a) Standing-Fall in LOS, (b) Walking-Fall in LOS, (c) Standing-Fall in NLOS, and (d) Walking-Fall in NLOS.

singling out the real fall from all of these activity combinations is very difficult, or even impossible.

Previous work [29] did make use of the above feature for real time activity segmentation, which was termed as Anomaly Detection. However, we argue that it oversimplifies the problem in two aspects, which limit its applicability: *First, the subject was assumed to stay in a controlled environment where only a few predefined activities were performed.* Hence when various undefined human activities are performed, the system will fail. *Second, two predefined activities should be separated by an immobile activity in between.* In other words, the subject cannot perform activities in a natural and continuous manner, e.g., one cannot stand up from the chair and walk, instead, he should stand up first, stand there for a while, and then walk. The limitations of the CSI amplitude motivate us to explore if we can find a better base signal for activity segmentation and fall detection.

4.2 Human Activities and Phase of CSI

As human activities can cause channel distortion which also leads to signal phase shift, so we follow the same logic of the last section to study the relationship between human activities and the phase information of CSI.

4.2.1 Phase Calibration

As mentioned in [40], the measured phase $\hat{\phi}_f$ of CSI of subcarrier f can be computed as follows:

$$\hat{\phi}_f = \phi_f + 2\pi f_f \Delta t + \beta + Z_f,$$

where ϕ_f is the true phase, Δt is the time lag at the antenna, β is an unknown constant phase offset, Z_f is some measurement noise, f_f is the carrier frequency offset at the receiver.

We find that the raw phases provided by commodity Intel 5300 NICs are randomly distributed and not usable, the reason lies in the term $2\pi f_f \Delta t$, since Δt is different across subsequent packets. Recent work [41] shows that on a single commodity wireless NIC, the RF oscillators are frequency locked at startup. So the f_f across different antennas on the same NIC is actually the same value. This inspires us to compute the phase difference $\Delta\phi_f$ between two antennas as:

$$\Delta\hat{\phi}_f = \Delta\phi_f + 2\pi f_f \varepsilon + \Delta\beta + \Delta Z_f,$$

where $\Delta\phi_f$ is the true phase difference, $\varepsilon = \Delta t1 - \Delta t2$ ($\Delta t1$ and $\Delta t2$ are time lags at the antenna 1 and 2 respectively). $\Delta\beta$ is the unknown constant phase difference offset, ΔZ_f is still the measurement noise. If we put two receiver antennas at the distance around $\frac{1}{2}\lambda$ from each other, ε indicates the propagation time of the distance difference Δd (which is around $\frac{1}{2}\lambda \sin\theta$) between two antennas. Then ε can be roughly estimated as follows: [42]

$$\varepsilon \approx \frac{1/2\lambda \sin\theta}{cT} \leq \frac{1}{2Tf},$$

where λ is the wavelength, f is the central frequency, c is the speed of light, T is the sample interval which is 50 ns in WiFi and θ is the direction of arrival. As we select the WiFi setting running on 5 GHz frequency, ε is thus approximately equal to zero. Thus, we get the measured phase difference $\Delta\phi_f$ as

$$\Delta\hat{\phi}_f = \Delta\phi_f + \Delta\beta + \Delta Z_f.$$

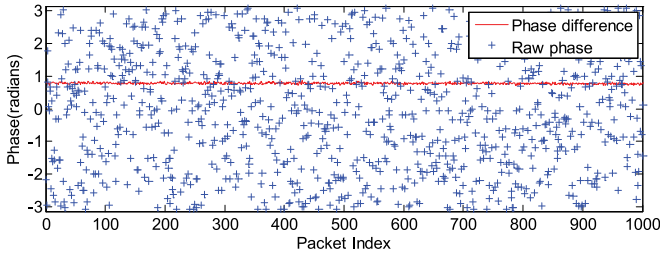

Fig. 5. Raw Phase versus Phase Difference without human presence.

Fig. 5 shows the raw randomly distributed phase and the phase difference in a no human presence environment respectively. We can see that the randomly distributed raw phase can be calibrated by conducting phase difference over a pair of antennas. In the following sections, we conduct experiments to see the relationship between human activities and the phase difference of CSI as we did for the amplitude.

4.2.2 Phase Difference Across Different Subcarriers and Streams

We have the similar observation for the phase difference as for the amplitude that human activities affect different subcarriers in a similar way and adjacent subcarriers behave similarly. From the CSI stream perspective, as the variances of the phase difference across two antennas is the sum of individual variance on each antenna,[1] which implies that the phase difference is more sensitive to the environment changes than the amplitude, thus the CSI phase difference seems to be a better base signal compared to the CSI amplitude for characterizing human activities.

4.2.3 Impact of Different Human Activities

Now we observe the phase difference caused by immobile and motion activities, respectively.

Impact of immobile human activities. As illustrated in Figs. 6a and 6c, immobile activities such as sitting and lying, result in relatively stable signal change patterns in time domain. One new observation is that the CSI phase difference signal fluctuates with the tiny human body movement.

1. PhaseU [42] gives detail proofs about this conclusion, we refer interested readers to that work for further information.

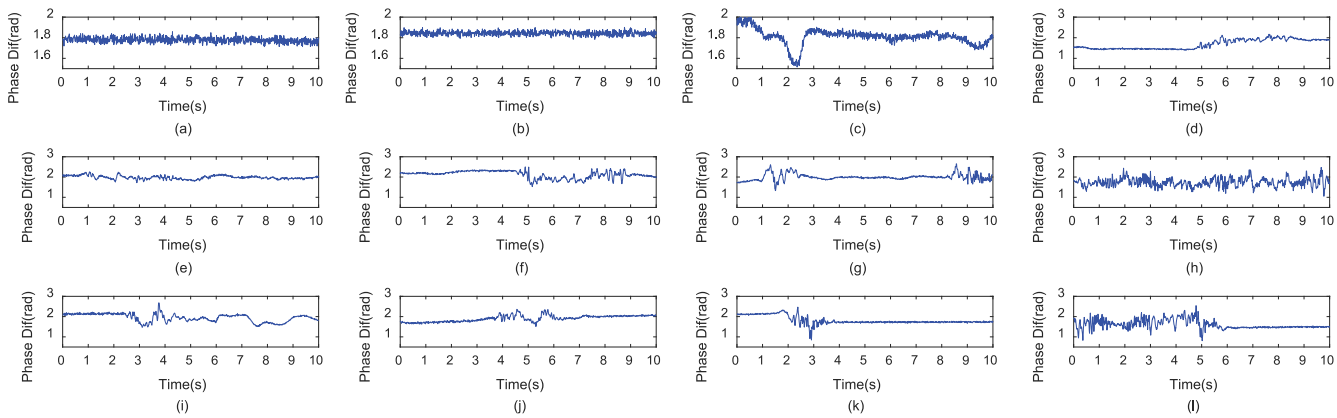

Fig. 6. Phase difference of human motion activities: (a) Sitting, (b) Lying, (c) Standing, (d) Lie down, (e) Upper body activities, (f) Pickup, (g) Squat, (h) Walking, (i) Stand up, (j) Sit down, (k) Standing-Fall, and (l) Walking-Fall.

Specifically, *the CSI phase difference during standing shows an obvious fluctuation compared to that caused by sitting and lying, and we can see a clear difference between their patterns.* As we also note that the boundary blurs as a subject is standing far away from LOS path. Hence, we cannot jump to a conclusion that the phase can reliably distinguish between the standing activity and other immobile activities.

Impact of human motion activities. Compared to immobile activities, motion activities lead to obvious CSI signal fluctuation in the time domain as illustrated in Figs. 6d and 6l. Again, there is still no obvious pattern to differentiate the real fall from other non-fall daily activities.

4.2.4 Activities in LOS and NLOS Conditions

Not surprisingly, as illustrated in Fig. 7, the phase variance caused by human activities becomes weaker from LOS to NLOS conditions. Now we answer the previous two questions with respect to phase difference.

With the setting we adopt, the answer to the first question is around 3.5 m in a clear environment and it drops to 3 m with a 1 m high wooden desk and an LCD desktop screen on it as an obstacle between the LOS and the human object as we did in Section 4.1.3. Compared to the amplitude, it seems that the CSI phase difference variance for the standing posture in both LOS and NLOS scenarios is amplified and the difference between the signal pattern of the standing and that of immobile activities becomes clearer. As the coverage area is enough for rooms with standard sizes, we argue that *the phase difference over two antennas proves to be a robust base signal to distinguish between lying (sitting) and standing*. The answer to the second question is 6 m without obstacles from LOS path but it drops to 5 m with the same desk as an obstacle. Considering the symmetry of both sides from LOS path, we conclude that *the phase difference is also a better base signal than the amplitude to distinguish the motion activities from immobile ones in common living rooms.*

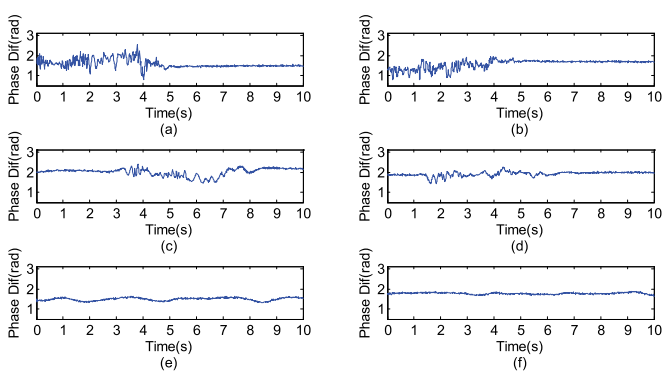

Fig. 7. Phase difference of activities in LOS and NLOS conditions: (a) LOS Walking-Fall, (b) NLOS Walking-Fall, (c) LOS Sit down, (d) NLOS Sit down, (e) LOS Standing, and (f) NLOS Standing.

4.2.5 Fall in Different Scenarios

As illustrated in Fig. 8, while most of the human activities, such as walking, running, standing and falling, all lead to obvious CSI phase difference fluctuation over time. Only several immobile activities, such as sitting still and lying, result in very steady and stable signal pattern over the time. In our previous work [31], it was found that only when people fall down, lie down and sit down, the variance of the phase difference exhibits an obvious transition from the fluctuation state to the stable one, and then the state transition of the CSI phase difference was used for real-time activity segmentation.

Through extensive experiments, the state transition of the CSI phase difference variance proves to be a robust feature in time domain to segment all the fall activities from the continuously received CSI streams. However, many "in-place" activities besides falling down, lying down and sitting down might also cause the state transition of the CSI phase difference, which leads to a lot of activities segmented out. Here "in-place" means the subject is conducting certain limb motions while lying or sitting. The transition happens

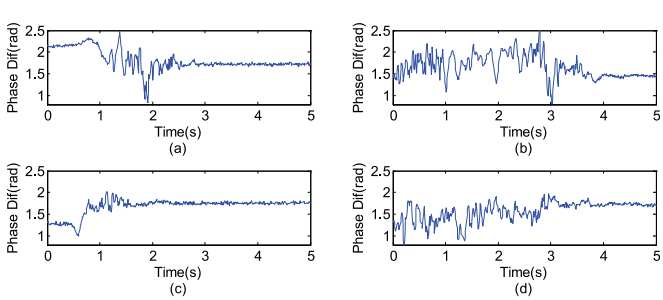

Fig. 8. Fall in different Scenarios: (a) Standing-Fall in LOS, (b) Walking-Fall in LOS, (c) Standing-Fall in NLOS, and (d) Walking-Fall in NLOS.

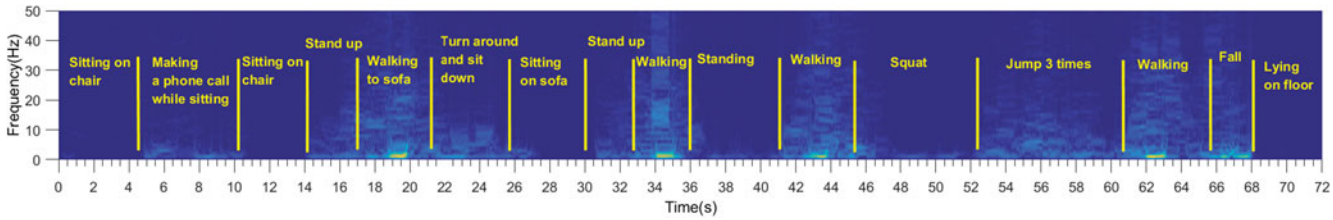

Fig. 9. Spectrogram for a series of different activities.

when the subject finishes certain in-place activities (such as eating, writing or making a phone call) and returns to the immobile postures. As there are different kinds of in-place activities, collecting all these activities for training and testing one by one for classification is difficult.

4.2.6 Power Profile versus Daily Activities

In order to reveal more effective features for fall segmentation and detection, we further use the Short-Time Fourier Transform to profile the spectrogram of the CSI phase difference signal corresponding to various daily activities. As shown in Fig. 9, it is interesting to see that different activities have different power profiles and the frequency range contributing to the power profile exhibits certain patterns. Specifically, we notice that:

1) The immobile postures such as sitting still (0-4 s, 11-14 s, 27-30 s) and lying still (68-72 s) have a weak power profile, as there is no any obvious body movement.
2) The "in-place" activities such as making a phone call while sitting (4-10s) and standing (36-41 s) have a mild power profile contributed mainly by the low frequency components (<5Hz), which are generated mainly the limb movement.
3) All the motion activities such as walking (17-21 s, 33-36 s, 41-46 s, 61-65 s), standing up (14-17 s), jumping (53-61 s), turning around and sit down (21-26 s), and falling (66-68 s) have a strong power profile with both low frequency [0, 5 Hz] and high frequency components (>5 Hz), which are generated by both limb and torso movement.
4) While the falls and sitting/lying down activities show a sharp power profile decline from high frequency to low frequency components (68 s, 25 s), the "in-place" activities won't cause such a sudden power profile decline as the power profile of "in-place" activities mainly lies in the low frequency range (<5 Hz).

Hence, by detecting the state transition of the CSI phase difference variance along with the sharp power profile decline pattern, we can robustly rule out the "in-place" activities but segment only the fall and a few other non-fall activities (i.e., lying down and sitting down). We refer those few other non-fall activities as *fall-like activities*.

Zooming in the power profile of the fall and fall-like activities, it is noticed that while the fall and fall-like activities both end up with a sharp power profile decline, the falls often exhibit even a sharper power profile decline pattern than the fall-like activities. For example, as shown in Fig. 9, comparing the power profile before and after the ending point of the fall (at 68 s), and that of the sit down activity (at 25 s), we can see that the fall shows an obvious sudden power decline from high frequency to low frequency components, whereas the sit down activity only shows a mild one. This unique characteristic of fall is probably caused by the uncontrollable state of the subject, because when a person falls, she would lose control of the body and experiences an accelerated moving stage before hitting the floor. As the subject hits the floor, the moving speed of the body would change from high to zero, without a controlled de-accelerating stage like other fall-like activities such as sitting down.

However, we also notice that this gap becomes closer with the speed of the fall-like activity increasing, i.e., the power profile decline pattern of some quick fall-like activities looks similar to that of the fall. In particular, when the speed of the fall-like activities increases to a comparable one with that of the falls, we can no longer tell the difference only by comparing the power profile decline pattern.

4.3 Summary

In this section, we conduct extensive experiments to study how the amplitude and phase difference of the CSI change in the presence of different human activities at indoor environment. As previous work only exploits the amplitude information, we start from that and find that the CSI amplitude can only tell whether a subject is performing motion activities or not. This can be useful for activity segmentation with simplified assumptions made in previous work [29]. However, it can not work well when various daily activities are performed naturally and continuously. The limitations of the CSI amplitude motivate us to explore the phase information in human activity recognition. Unfortunately, we observe that the raw phases provided by commodity WiFi devices are randomly distributed and thus not usable. After analyzing the reason, we take the phase difference across a pair of receiver antennas for phase calibration. Interestingly, we observe that the phase difference is more sensitive than the amplitude, further more, it can distinguish standing from other immobile activities such as sitting and lying. Based on this observation, our previous work proposed a simple transition based segmentation method, expecting to single out only the fall and a few fall-like activities (i.e., sitting and lying) in the continuously captured CSI streams. However, we found that some "in-place" activities may also be segmented out as fall-like activities, which lead to difficulties in accurate fall detection. Fortunately, we find the sharp power profile decline pattern, which is always associated with fall and fall-like activities, but not with "in-place" activities. Furthermore, we also see that the power profile decline patterns of the fall and fall-like activities often look quite different. Thus, by combining the state transition of

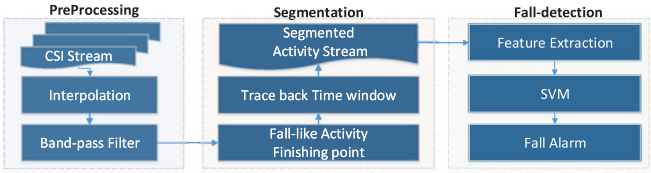

Fig. 10. The RT-Fall system framework.

the CSI phase difference variance with the sharp power profile decline pattern, we not only resolve the "in-place" activity issue for segmentation, but also provide new clues for fall detection.

5 Framework & Methodology

Our proposed real-time and contactless fall detector, RT-Fall, consists of three functional modules: *signal preprocessing*, *fall-like activity segmentation* and *fall detection*. As shown in Fig. 10, the system takes the CSI signal streams as input, which can be collected at the receiver side using two receiver antennas of a commodity WiFi device (e.g., Intel 5300 NIC). Each CSI signal stream contains CSI readings from 30 subcarriers on a wireless stream and totally two CSI streams are collected in the experiment between one transmitter antenna and two receiver antennas. The CSI sampling rate is set to $100\ pkts/s$ as [29]. The system can take advantage of CSI measurements from existing traffic across these links, or if insufficient network traffic is available, the system might also generate periodic traffic for measurement purposes.

5.1 Signal Preprocessing

The goal of signal preprocessing is two-fold: 1) dealing with the uneven arrival of packets caused by the bursty Wi-Fi transmissions to make the signal stream continuous for further signal processing; 2) filtering out signal noises which won't contribute to fall segmentation and detection. The above two goals are achieved by applying the following two techniques: interpolation and band-pass filtering.

5.1.1 Interpolation

Wi-Fi is a shared channel, where multiple devices use random access to share the medium. This results in the received packets that are not evenly spaced in time domain. Two problems may occur if the arrival of packets is not evenly spaced: 1) the sampled CSI readings during the fall may not be continuous, which makes it difficult for feature extraction; 2) unevenly spaced samples in time domain prevent Time-Frequency analysis to obtain the spectrogram. To get evenly spaced samples, we adopt the 1-D linear interpolation algorithm as suggested in [43] to process the raw CSI readings.

5.1.2 Band-Pass Filter

The interpolated CSI signal stream is then fed into a band-pass filter to further rule out irrelevant signal frequency components. As the speed of chest movement caused by respiration or slight body movement are relatively low compared to that of the fall, the signal changes caused by these motions mainly lie in the lower frequency range, often within [0, 4 Hz]. Furthermore, these body motions are embedded in all the human activities. Hence, it is reasonable to conduct a band-pass filter to filter out the signal components which are below the frequency of 4 Hz. Through experiments, we find the frequency range that can filter-out the non-relevant activities yet well characterize the fall and fall-like activities lies in [5, 10 Hz].

5.2 Activity Segmentation

The main function of the activity segmentation module is to single out the fall and fall-like activities from the continuously received CSI streams. It consists of two steps: in step one, the finishing point of the fall or fall-like activities is identified automatically by processing the variance of CSI phase difference; then in step two, the starting point of the fall or fall-like activities is determined by selecting a proper trace back window size from the finishing point.

5.2.1 Identify the Finishing Point of Fall or Fall-Like Activities

In the empirical study section, it was found that the state transition of the CSI phase difference variance is a robust base signal to detect the fall and fall-like activities (i.e., lying down, sitting down). Based on the two observations described previously, we propose a two-phase segmentation approach to separate the fall and fall-like activities from other activities in the continuously received CSI streams.

In phase one, we use a threshold-based sliding window method to determine if the raw phase difference signal and the band-pass filtered phase difference signal are in the fluctuation state or stable state. This process consists of three steps: First, we collect the two signal streams in stable state (e.g., lying/sitting in LOS path) across multiple sliding windows off-line and calculate their mean μ and the normalized standard deviation σ, respectively; Then, we determine the threshold value δ for both signal streams as: $\mu + 6\sigma \leq \delta$. In the last step of phase one, we acquire the two signal streams in a sliding window on-line as shown in Fig. 11b and see if they are in the fluctuation state or stable state, by comparing the mean value in the sliding window with the threshold δ. If the mean value is smaller than δ, the signal is said to be in the stable state, otherwise it is in the fluctuation state.

In phase two, we detect the transition from the fluctuation state to stable state for both the raw phase difference signal and the band-pass filtered phase difference signal, and determine the finishing point of the fall and fall-like activities by checking if both signals enter the stable state. The process contains two steps: In step one, we keep tracking of the state of two signals and checking if there is a transition occurring from the fluctuation state to stable state. When such a transition happens, we mark the time $t1$ as shown in Fig. 11b and start monitoring the state of the other signal. If the other signal also enters the stable state within a timelag Δt from $t1$, we mark the instant $t2 = t1 + \Delta t$ as the finishing point of the fall and fall-like activities.

The rationale behind detecting the two signal state transitions for the fall and fall-like activity segmentation is that we detect the CSI phase difference transition as the first

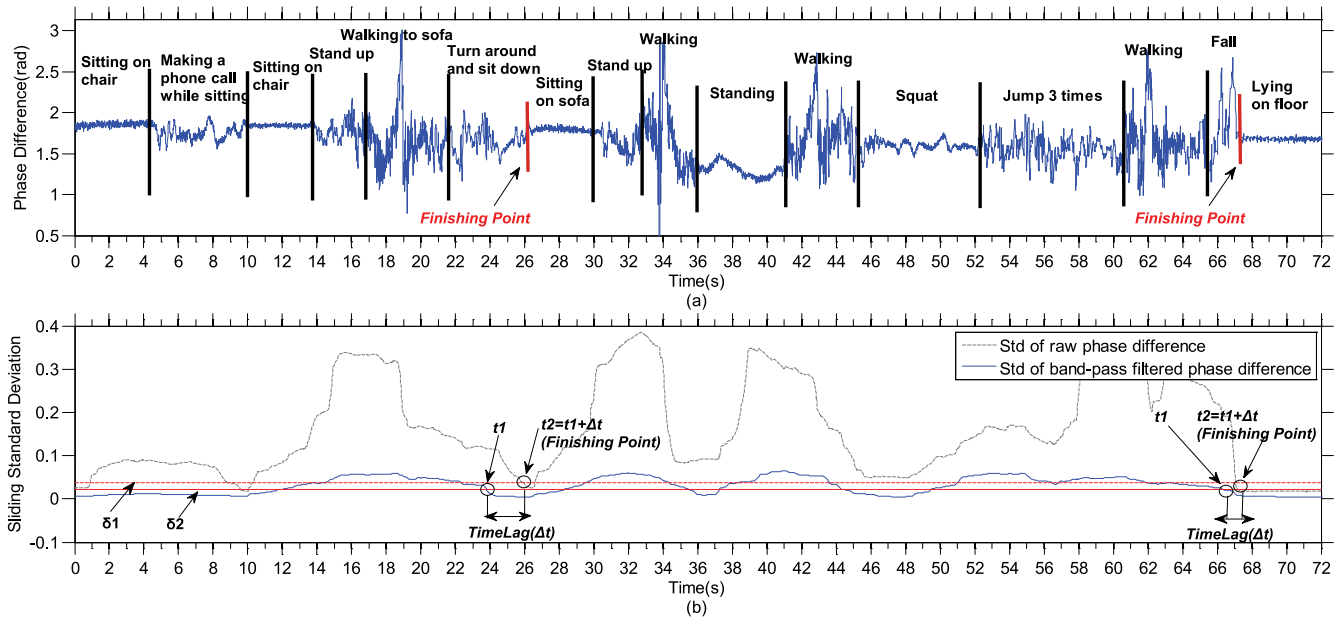

Fig. 11. Fall and fall-like activity finishing point identification: (a) Phase difference across a continuously performed activities. (b) The corresponding sliding standard deviation of (a). $\delta 1$ and $\delta 2$ are the thresholds for the raw and band-pass filtered phase difference, respectively.

criteria and then filter out the "in-place" activities by checking the band-pass CSI phase difference variance. If we only track the state transition of the raw phase difference variance as we did in our previous work [31], the "in-place" activities may also be segmented out as fall-like activities. As shown in the grey-dashed line of Fig. 11b, when the subject stops making a phone call, the raw phase difference shows a state transition (at 9 s), which meets our previous segmentation criteria. If we only track the state transition of the band-pass filtered CSI phase difference variance, we will no longer distinguish the lying (sitting) from standing, as the energy-band caused by standing activity lies in the same frequency range as for the in-place activities. As shown in the solid-blue line of Fig. 11b, when the subject finishes walking and then stands still, the band-pass filtered phase difference shows a transition (at 36 s) from the fluctuation state to stable state. As the fall is always accompanied by a CSI phase difference state transition and a sharp power profile decline where the energy from the high frequency to low frequency components all drops within a very short period of time, which inspires us to track the state transitions of both signals as well as the time lag. In particular, the shorter the Δt is, the sharper the power profile decline is.

As shown in Fig. 11a, we depict the CSI phase difference of a series of activities performed continuously and label the corresponding activities. While Fig. 11b shows the fall and fall-like human activity finishing point identification results based on our two-phase segmentation approach. It can be seen that only the fall and fall-like activities are identified, while other activities such as making a phone call, standing up and walking are left out.

5.2.2 Determine the Proper Trace Back Window Size for Fall-Detection

Based on the CSI phase difference state transition detection, we can identify the finishing point of fall and fall-like activities in the continuously captured WiFi signal streams. To differentiate the fall from fall-like activities, we need to decide the proper trace back window size to collect training data samples for accurate fall detection. The window sizes tested in previous fall detection work were ranging from 0.32 s [44], 1 s [45], to 10 s [46] according to the adopted sensors and fall detection methods. Considering the duration and characteristics of the fall and other fall-like activities in time domain, we perform intensive experiments to choose the best window size with trial-and-error method. It was found that the best window size is three seconds, composing a two-second signal segment before the finishing point and a one-second signal segment after, representing the whole segmented activity stream.

5.3 Fall Detection

After determining the starting and finishing point of the fall and fall-like activities, only the CSI phase difference and amplitude of those activities are singled out. The goal of the Fall Detection module is to separate the fall from fall-like activities.

5.3.1 Feature Extraction

Through extensive study, we extracted the following eight features from the real time captured CSI streams for activity classification: (1) the normalized standard deviation (STD) of CSI, (2) the median absolute deviation (MAD), (3) the offset of signal strength, (4) interquartile range (IR), (5) signal entropy, (6) the velocity of signal change, (7) the TimeLag, (8) the power decline ratio (PDR). As the first six features are used and explained in [29] for activity classification, here we only elaborate the two new features.

Both TimeLag and PDR are proposed based on the observation that the fall and fall-like activities are different from the signal power profile perspective. TimeLag characterizes the time delay of the state transition point between the band-pass filtered and the raw phase difference as shown in Fig. 11b, we can see that the time lag for the fall is usually much shorter than that of the sit down activity. If we compute the one-second accumulated power before and after

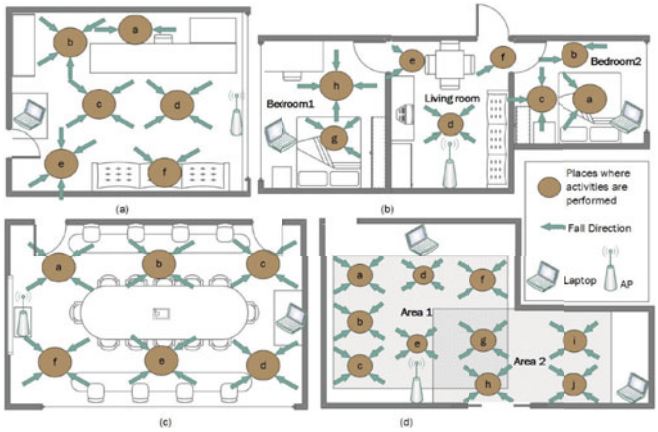

Fig. 12. Four test environments: office (a), Apartment (b), Meeting Room (c), and Hall (d).

the finishing point, then the PDR is defined as the power decline ratio which is the one-second power loss divided by the one-second accumulated power before the finishing point. PDR is computed with the following mathematical formula:

$$PDR = \frac{\sum_{t=\hat{t}_{-1}}^{\hat{t}} \sum_{f=f_l}^{f_h} e_{t,f}\omega_f - \sum_{t=\hat{t}}^{\hat{t}_{+1}} \sum_{f=f_l}^{f_h} e_{t,f}\omega_f}{\sum_{t=\hat{t}_{-1}}^{\hat{t}} \sum_{f=f_l}^{f_h} e_{t,f}\omega_f},$$

where $\hat{t}$ is the finishing point, $\hat{t}_{-1}$ is the instant of one second before $\hat{t}$ and the $\hat{t}_{+1}$ is that of one second after $\hat{t}$. f_l and f_h refer to the frequency range from [0, 50 Hz]. $e_{t,f}$ is the power strength of a specific frequency f at a specific time t. ω_f is the weight vector for each frequency f.

Different from WiFall [29] that only extracts features from the CSI amplitude information, we extract the first six features from *both CSI amplitude and phase difference*, and extract the two new features from *phase difference* only. They together constitute the input of the SVM Classifier.

5.3.2 SVM Classifier

To detect the fall among the segmented activities, the ν-SVM classifier [47] is applied using the features extracted above. All the samples are divided into objective class (i.e., the fall) and non-objective class (i.e., fall-like activities). To solve the non-linear classification problem, it maps input samples into a high dimensional feature space by using a kernel function and finds the maximum margin hyperplane in the transformed feature space. The SVM classifier requires a training dataset and test dataset. In the process of classification model construction, fall and fall-like activities are segmented and labeled in the continuously captured WiFi wireless signal streams in the activity segmentation phase. Then the extracted features along with the corresponding labels are fed into the SVM classifier to build the classification model. In the process of real-time fall detection, the classification results along with the data samples will be recorded. With the user feedback, the wrong classification results will be re-labeled correctly and the model updating process will be triggered in time to update the classification model. We create the ν-SVM classification model by utilizing LibSVM [48] with the Gaussian Radial Basis Function (RBF) kernel chosen and set the parameter ν to be 0.5, which indicates the upper bound on the fraction of training errors and the lower bound of the fraction of support vectors, leaving other parameters as default.

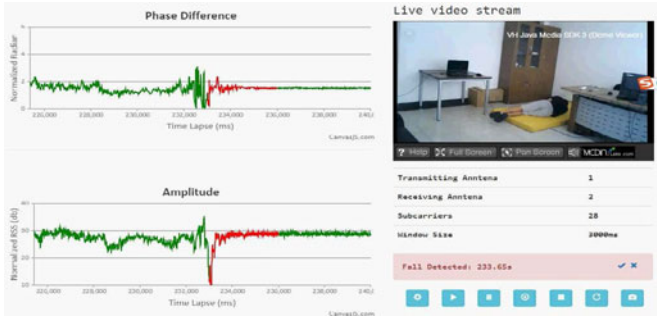

Fig. 13. User interface.

6 Evaluation

In this section, we present the implementation and evaluation results of our RT-Fall system using commercial off-the-shelf WiFi devices.

6.1 Experimental Setups

We evaluate our RT-Fall system using an 802.11n WiFi network consisting of one or more off-the-shelf WiFi devices (laptop or mini-pc) and a commodity wireless access point (i.e., TP-Link WDR5300 Router with one antenna running on 5 GHz). The laptop/mini-pc is equipped with an Intel WiFi Link 5,300 card for measuring CSI [21] and with two internal antennas. The packet transmission rate is set to $100pkts/s$.

We conduct experiments in four different environments to show the generality of our system. The experimental setup and settings in these environments are shown in Fig. 12. The first test environment (i.e., office) has the size of about $3\,\mathrm{m} \times 4\,\mathrm{m}$ with one sofa, two tables and one bookcase (see the photo inside Fig. 13); the second test environment is an apartment with two bedrooms and one living room, equipped with a group of sofas, two tables and two beds; the third test environment (i.e, meeting room) is about $6\,\mathrm{m} \times 6\,\mathrm{m}$ with a long meeting table and dozens of chairs around, the fourth one is a big hall with the size of $12\,\mathrm{m} \times 6\,\mathrm{m}$.

6.2 Dataset

We recruit 6 volunteers (five male and one female; age: 21-32 years; height: 1.6-1.83m; weight: 61-82 kg) to perform various daily activities in the four test environments over two months. Each data record consists of a continuous stream of activities, mixing the fall, fall-like and other daily activities. These activities include the specified Activities of Daily Living(ADL) summarized in [20] (e.g., standing, walking, running/jogging, jumping, sitting down, getting up from chair/bed, lying down, picking up object, ...) and other common activity types (e.g., answering phone, eating, performing exercise like push-up). We let the subjects to fall naturally but provide a mattress to protect the subjects from being injured. Specifically, the subjects performed the fall according to their experiences to simulate the sudden loss of balance, including forward, backward, sideward and

	Classified as Fall	Classsified as not Fall
Is Fall	TP (True Positive)	FN (False Negative)
Is not Fall	FP (False Positive)	TN (True Negative)

Fig. 14. Confusion matrix.

backward fall while walking or standing.[2] We install a camera in each room to record the activities conducted as the ground truth. The web-based user interface of our system is shown in Fig. 13, where the recorded video, the amplitude and phase difference of CSI, the segmented activity from CSI stream, and the detection results are updated on-line in real-time. When the system is started, a subject can perform any activities naturally and continuously,[2] and the system will automatically segment CSI streams and report the segmentation/detection results in real-time on the user interface. Based on the recorded activity video and detected results, it is very easy for the user to report the test results, ranging from the number of falls performed and detected, to the fall-like activities performed and detected. In all the following sections, we let subjects to perform activities, and ask a separate student to record the full experiment results for performance evaluation purposes.

6.3 Baseline Method and Performance Metrics

In the experiments, we use the state-of-art fall detector WiFall proposed in [29] as the baseline. *Since WiFall cannot segment the fall and other daily activities reliably, we thus leverage our proposed method to segment the fall and fall-like activities*, subsequently we compare its activity classification performance with that of our approach using our dataset. We use the following two standard metrics for performance evaluation—*sensitivity* and *specificity*. The confusion matrix is shown in Fig. 14 to define sensitivity and specificity.

Sensitivity is defined as the percentage of correctly detected falls: $sensitivity = TP/(TP + FN)$

Specificity is defined as the percentage of correctly detected non-fall activities: $specificity = TN/(TN + FP)$.

6.4 System Performance and Number of Participants

As different people perform activities in different ways, for example, some sit down faster, while some fall slower, thus we design a set of experiments in the office room to see how many subjects' training data is sufficient for obtaining stable and satisfactory test results, through testing the system performance with increasing the number of participants involved. Considering that the activities can occur in different places and from different directions as shown in Fig. 12a, we ask the participants to evenly cover all the situations when they perform experiments.

As shown in Fig. 15a, the experiments consist of two phases: training data collection phase and testing phase. In the training data collection phase, we collect the training dataset by increasing the number of participants involved, each subject conducts 100 falls and fall-like activities respectively,

2. A demonstration video has been recorded and uploaded to YouTube (please see: https://youtu.be/WgTnKjr5xow) and Youku (see: http://v.youku.com/v_show/id_XMTQ1NDg1ODIyOA==.html?from= s1.8-1-1.2) to show how various activities and falls are conducted in the natural setting.

Experiment Group	Training Data Set	Training Data Collection Phase					Testing Phase				
		Subject	Time expense (h)	Time span (day)	Fall	Fall-like	Subject	Time expense (h)	Time span (day)	Fall	Fall-like
	empty	a	6	2	100	100					
M{a}->a	a						a	4	2	40	80
M{a}->b	a						b	3	1	40	80
	a	b	9	3	100	100					
M{a,b}->b	a,b						b	3	2	40	80
M{a,b}->c	a,b						c	3	1	40	80
	a,b	c	8	3	100	100					
M{a,b,c}->c	a,b,c						c	3	2	40	80
M{a,b,c}->d	a,b,c						d	3	1	40	80
M{a,b,c}->e	a,b,c						e	2	1	40	80
M{a,b,c}->f	a,b,c						f	2	1	40	80

(a)

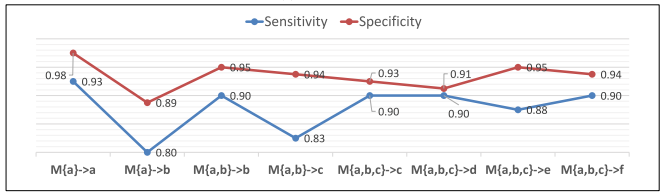

(b)

Fig. 15. System performance and Number of Participants: (a) Experiment design. (b) Performance evaluation with different number of people. $M\{S\} -> x$ means building the model $M\{S\}$ from the training data of the people set S to evaluate the performance with the dataset of user x.

and the system uses the training data from the subject set S to build the model $M\{S\}$. In the testing phase, each subject x conducts 40 falls and 80 fall-like activities respectively to evaluate the performance using the model built from the training data of the subject set S, and the evaluation results of each experiment group are shown in Fig. 15b, where the classification model M is built with the training dataset and the tests are done using those models for different number of participants. For example, at the beginning, as the training data set is *empty*, we collect training data from the first subject a to build a model $M\{a\}$ (see first row in Fig. 15a), which refers to the model built with one participant's dataset (user a performed 100 falls and 100 fall-like activities, spending 6 hours in 2 days' time), and then test the performance on subject a using model $M\{a\}$ from the training data of himself (see second row: $M\{a\} \rightarrow a$). Then the second subject participates in the experiments to evaluate the performance using the model $M\{a\}$ (see third row: $M\{a\} \rightarrow b$) to see if we can get consistent performance as the first subject. If not, we go on collecting training data from the second subject (see fourth row) to increase the training data set and build the model $M\{a, b\}$, and so on so forth, until we get roughly consistent performance with the smaller training dataset.

According to Fig. 15b, $M\{a\} \rightarrow a$ has the best result, but it lacks generality to detect falls of other people accurately; with the number of participants increasing to three, the performance obtained with the model built from three subjects' training data tends to converge, which is a little lower than that of $M\{a\} \rightarrow a$. This is expected because $M\{a\} \rightarrow a$ corresponds to a personalized model, whereas $M\{a, b, c\}$ corresponds to a generalized one that is trained for more people. Furthermore, according to the videos recorded, in the training and testing phases, all the 620 falls are 100 percent segmented out. Averaging the performance of the last three experiment groups, i.e., $M\{a, b, c\} \rightarrow d, e, f$, we achieve 93 percent of sensitivity and 89 percent of specificity in the office room. In the rest of this section, *we use the generalized model built from three subjects' training data for further evaluation*.

Test Rooms	Training Data Collection Phase					Testing Phase				
	Subject	Time expense (h)	Time span (day)	Fall	Fall-like	Subject	Time expense (h)	Time span (day)	Fall	Fall-like
Office (R1)	a,b,c	-	-	300	300	d,e,f	-	-	120	240
Apartment (R2)	a,b,c	51	14	300	300	d	3	3	40	80
						e	2		40	80
						f	2		40	80
Meeting Room (R3)				300	300	d	3	2	40	80
						e	2		40	80
						f	2		40	80
Hall (R4)				300	300	d	2	2	40	80
						e	2		40	80
						f	2		40	80

(a)

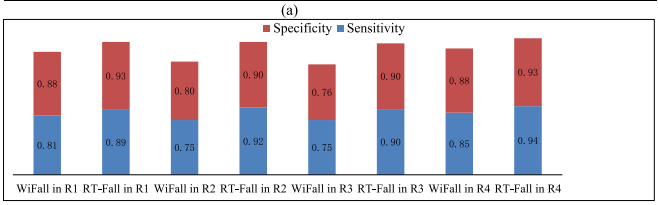

(b)

Fig. 16. Performance comparison in different rooms: (a) Experiment design. (b) Performance results.

6.5 System Evaluation and Comparison

In this part, we first compare the performance of RT-Fall with that of the baseline method WiFall [29] in four different test environments, in terms of sensitivity and specificity. Then, we evaluate the system robustness of RT-Fall system with respect to various environment changes.

6.5.1 Performance Comparison

We design experiments in four test environments as shown in Fig. 16a to compare the performance of RT-Fall with that of the baseline method WiFall [29]. As we have already collected training and testing data in Section 6.4 in the office room, we spent two weeks in an apartment, meeting room and the hall again with the three students (a,b,c) in the training data collection phase. In the office room and the meeting room, as we only need one AP and one WiFi device to cover the whole area, two classification models were built for each room, one is based on our approach, the other is based on WiFall. *However, in the apartment and the big hall, we need one AP and two WiFi devices to cover the whole area* as shown in Fig. 12. Specifically, in the apartment, we train three classification models from the training dataset, each model corresponding to one room. To make the three models work together, the CSI captured in two WiFi devices were synchronized to a central sever. As each room has its own model, the system needs to track which room the subject is in to select the proper model to use. Actually it is quite simple for RT-Fall to detect this. For example, if the subject is in the living room, the CSI phase difference signals in both WiFi devices are in unstable state. However, if the subject is in one of the two bedrooms, only the WiFi device closer to the subject has unstable CSI phase difference signal while the other one has stable signal. In the hall, as the area is too large for only one AP and one WiFi device to cover, we deploy two WiFi receiving devices. Again, two classification models were built for two separate areas and the CSI captured in two WiFi devices were synchronized to make the final decision. As each area has its own model, the system also needs to track which area the subject is in. RT-Fall leverages the fact that when the subject is close to one WiFi device, the standard deviation of the CSI phase difference in this WiFi device will show severer fluctuation than that of the other WiFi device. Knowing this information is tantamount to knowing which area the subject is in. In the testing phase, three different students (d, e, f) were invited to perform daily activities and evaluate the performance of these models built from the training data set with the subject set (a, b, c). Averaging the evaluation results with the three students for each room, we get the performance comparison results in Fig. 16b. In general, RT-Fall achieves 91 percent of sensitivity and 92 percent of specificity. Compared to the baseline method WiFall, RT-Fall gets 14 percent higher sensitivity and 10 percent higher specificity.

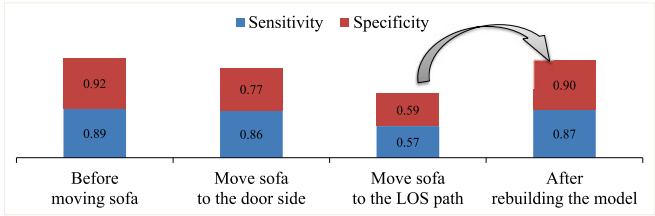

Fig. 17. Robustness to furniture location change.

6.5.2 Robustness

As wireless signal is said to be very sensitive to environment, we thus evaluate the robustness of our approach against setting changes, including opening the door and window, switching on/off the light, moving the furniture around, and testing in different rooms. While the RT-Fall system performance is not affected much by the opening of windows/door or the light on/off in the four test environments, its performance deteriorates when the big furniture is moved or test is done in a new environment with the old model built for the old environment. We will detail the results in the following subsections.

Impact of moving the furniture location. We move the sofa to different places in the office room to evaluate the impact on the fall detection performance. The experiment was done under four different conditions: Fall detection is conducted while the sofa is put in the original place (baseline), perform the same experiment when the sofa is moved to the door side, do the same test after moving the sofa to the LOS path, and re-train the model and repeat the test as in last case. We arrange three students to conduct 20 falls and 40 fall-like activities in each of the first three scenarios to evaluate the impact on the system performance, and each student completes all the tests in one day. For the last test, we ask each student to conduct 100 falls and 100 fall-like activities in one week and use the collected training data to rebuild the model. Then we evaluate the new model in the same way as we did in the first three scenarios to get the averaged results as shown in Fig. 17. When the sofa is moved from the original place to the door side, the sensitivity drops a little bit from 89 to 86 percent and the specificity drops from 92 to 77 percent. However, when the sofa is moved to the room center which blocks the LOS path, the sensitivity suffers from a severe deterioration from 89 to 57 percent and the specificity drops from 92 to 59 percent. So it seems that the bulky furniture movement has quite a big impact on the fall detection results, the reason is probably due to the significant CSI change caused by the variations in RF propagation multi-paths. When the model was reconstructed using the

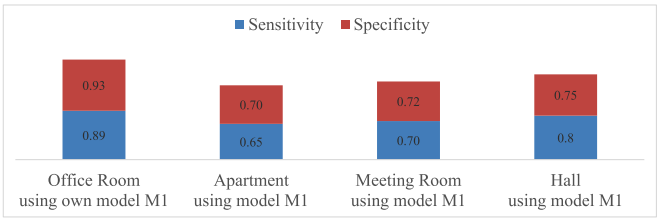

Fig. 18. Robustness to different rooms.

training data collected in the new setting, the test results restore to a comparable level, with 87 percent of sensitivity and 90 percent of specificity respectively.

System evaluation in different environments. Finally, we conduct experiments to test the performance of a model built for one environment in other environments. Specifically, we use the model $M1$ built for the office room and apply it to the apartment and meeting room settings. We ask three students to conduct 40 falls and 80 fall-like activities in each place in three days. Then we get the averaged results of system performance in each environment as shown in Fig. 18. The sensitivity changes from 89 to 65 percent, 70 and 90 percent in the apartment, meeting room and hall setting, respectively; and the specificity drops from 93 to 70 percent, 72 and 75 percent in the apartment, meeting room and hall setting, respectively. Finally, averaging the results in the apartment, meeting room and hall, the sensitivity drops from 89 to 71 percent while the specificity drops from 93 to 72 percent. If we recall the RT-Fall system performance in each place with the model constructed for that environment as shown in Fig. 16b, it is obvious that all the system models are environment dependent and optimal performance can be achieved only by fine-tuning the personalized model in a specific environment. In summary, the system is quite robust to small environment changes. For the significant environment changes, the system performance can be ensured by applying the new model learned from the changed settings.

7 Discussion

7.1 Major Reasons Causing Detection Errors

As the sensitivity and specificity are not 100 percent, we would like to analyze what causes the classification errors in fall detection. After careful analysis about the classification algorithms and results, we find two major reasons that prevent perfect fall detection. The first reason is that the features extracted for fall-like activities are very close to those of falls under certain context, which lead to wrong classification results in terms of both sensitivity and specificity. For example, when the subject quickly sits down onto the chair and leans against the back of the chair, it is sometimes classified as a fall. For this type of mis-classification, we plan to introduce more salient features as the input to help distinguish the fall and fall-like activities. The second reason is that the extracted features for fall and fall-like activities are context-dependent, the same type of activities may show different features for different places. Taking the office room (see Fig. 12a) as example, we notice that the locations behind the desk (a, b) have lower detection rate than locations in c, d, e, f. One possible reason is that there is a direct signal path between human body and the transceivers in c, d, e, f, but the direct signal path is blocked for the locations a and b. Hence a promising research direction is to introduce context such as location information in the fall detection algorithm to improve the system performance. For instance, we might roughly locate the elder in the room first, and then select a location-based classification model for accurate fall detection.

7.2 Extend the Solution to Multi-Room Settings

This work focuses mainly on the use case of applying the fall detection system in a single room setting. Even though we also test the RT-fall in an apartment with three rooms and obtain quite satisfactory results, we find that it's not trivial to find the best places to install the WiFi access point and device to ensure good RF coverage and consistent detection performance in a multi-room setting. In fact, it's rather a big challenge to find the optimal setting given a certain multi-room layout. In the future we plan to investigate the optimal device placement issue for RF coverage and fall detection.

7.3 Extend the Solution to Multi-Person Settings

Although RT-fall is designed for a single elder living alone and independently at home, we did perform experiments to see its applicability in multi-person settings. We find that RT-fall can work only when there is only one person moving while the others are still. Specifically, we find that if two subjects are in the room, one is sleeping or sitting on the chair, when the other subject falls, RT-fall can still detect it reliably. This corresponds to the situation that when one elder is sleeping during night, the system can still detect the fall when the other elder gets up and falls in the same apartment. While both elders are active, one should be able to help when the partner happens to fall in the same apartment.

8 Conclusion

In this paper, we design and implement a real-time, contactless, low-cost yet accurate indoor fall detection system, RT-fall, using one commercial off-the-shelf WiFi router and WiFi receiving devices. To the best of our knowledge, this is the first work to identify the CSI phase difference as a better base signal than amplitude for fall activity segmentation and detection, it also discovers the sharp power profile decline pattern of the fall in the time-frequency domain and leverages the insight for accurate fall segmentation/detection. Experimental results conducted in four indoor environments demonstrate that RT-fall has great potential to become a practical and non-intrusive fall detection solution.

Fall detection has long been a research challenge in the public healthcare domain for the elders. Although we implemented quite an effective fall detector using off-the-shelf WiFi devices, there are still many interesting problems that deserve further study. For example, can we develop a very accurate personalized fall detector for each individual elder? How can we develop a fall detector which can adapt and evolve according to the environment change? While in this work we exploit the power of phase difference for activity segmentation and fall detection, we believe that it could be an effective enabler for activity recognition in general, especially for those with tiny body movement. We are

working on these questions and expect to obtain promising results soon.

ACKNOWLEDGMENTS

This work is funded by the National 1000-plan Research Grant and the NSFC Grant No. 61572048. The authors would like to thank Wang Yibo, Li Xiang, and Wu Dan for their help with experiments. D. Zhang is the corresponding author.

REFERENCES

[1] S. R. Lord, C. Sherrington, H. B. Menz, and J. C. Close, *Falls Older People: Risk Factors Strategies Prevention*. Cambridge, U.K.: Cambridge Univ. Press, 2007.

[2] O. A. FALLS. (2013). Falls among older adults: An overview [online]. Available: http://www.cdc.gov/HomeandRecreationalSafety/Falls/adultfalls.html/

[3] P. J. Rajendran, "A smart and passive floor-vibration based fall detector," Ph.D. dissertation, Univ. Virginia, Charlottesville, VA, USA, 2007.

[4] D. Wild, U. Nayak, and B. Isaacs, "How dangerous are falls in old people at home?" *B. Med. J.*, vol. 282, no. 6260, pp. 266–268, 1981.

[5] S. M. Friedman, B. Munoz, S. K. West, G. S. Rubin, and L. P. Fried, "Falls and fear of falling: Which comes first? a longitudinal prediction model suggests strategies for primary and secondary prevention," *J. Amer. Geriatrics Soc.*, vol. 50, no. 8, pp. 1329–1335, 2002.

[6] H. Rimminen, J. Lindström, M. Linnavuo, and R. Sepponen, "Detection of falls among the elderly by a floor sensor using the electric near field," *IEEE Trans. Inform. Technol. Biomed.*, vol. 14, no. 6, pp. 1475–1476, Nov. 2010.

[7] Y. Li, K. Ho, and M. Popescu, "A microphone array system for automatic fall detection," *IEEE Trans. Bio. Eng.*, vol. 59, no. 5, pp. 1291–1301, May 2012.

[8] H. Foroughi, B. S. Aski, and H. Pourreza, "Intelligent video surveillance for monitoring fall detection of elderly in home environments," in *Proc. 11th IEEE Int. Conf. Comput. Inform. Technol.*, 2008, pp. 219–224.

[9] N. Noury, A. Fleury, P. Rumeau, A. Bourke, G. Laighin, V. Rialle, and J. Lundy, "Fall detection-principles and methods," in *Proc. 29th IEEE Annu. Int. Conf. Eng. Med. Biol. Soc.*, 2007, pp. 1663–1666.

[10] X. Yu, "Approaches and principles of fall detection for elderly and patient," in *Proc. 10th Int. Conf. e-health Netw., Appl. Serv.*, 2008, pp. 42–47.

[11] V. Spasova and I. Iliev, "A survey on automatic fall detection in the context of ambient assisted living systems," *Int. J. Adv. Comput. Res.*, vol. 4, pp. 94–109, 2014.

[12] C. D. Lord C.J., "Falls in the elderly: Detection and assessment," in *Proc. Annu. Int. Conf. IEEE Eng. Med. Biol. Soc.*, 1991, pp. 1938–1939.

[13] Q. T. Huynh, U. D. Nguyen, L. B. Irazabal, N. Ghassemian, and B. Q. Tran, "Optimization of an accelerometer and gyroscope-based fall detection algorithm," *J. Sens.*, vol. 2015, pp. 1–8, 2015.

[14] F. Bianchi, S. J. Redmond, M. R. Narayanan, S. Cerutti, and N. H. Lovell, "Barometric pressure and triaxial accelerometry-based falls event detection," *IEEE Trans. Neural Syst. Rehabil.*, vol. 18, no. 6, pp. 619–627, Dec. 2010.

[15] Y.-C. Chen and Y.-W. Lin, "Indoor RFID gait monitoring system for fall detection," in *Proc. IEEE 2nd Int. Symp. Aware Comput.*, 2010, pp. 207–212.

[16] J. Dai, X. Bai, Z. Yang, Z. Shen, and D. Xuan, "Perfalld: A pervasive fall detection system using mobile phones," in *Proc. 8th IEEE Int. Conf. Pervasive Comput. Commun. Workshops*, 2010, pp. 292–297.

[17] S. Tao, M. Kudo, and H. Nonaka, "Privacy-preserved behavior analysis and fall detection by an infrared ceiling sensor network," *Sensors*, vol. 12, no. 12, pp. 16920–16936, 2012.

[18] Z.-P. Bian, J. Hou, L.-P. Chau, and N. Magnenat-Thalmann, "Fall detection based on body part tracking using a depth camera," *IEEE J. Biomed. Health Informat.*, vol. 19, no. 2, pp. 430–439, Mar. 2015.

[19] E. E. Stone and M. Skubic, "Fall detection in homes of older adults using the microsoft kinect," *IEEE J. Biomed. Health Informat.*, vol. 19, no. 1, pp. 290–301, Jan. 2015.

[20] N. Pannurat, S. Thiemjarus, and E. Nantajeewarawat, "Automatic fall monitoring: A review," *Sensors*, vol. 14, no. 7, pp. 12900–12936, 2014.

[21] D. Halperin, W. Hu, A. Sheth, and D. Wetherall, "Tool release: Gathering 802.11 n traces with channel state information," *ACM SIGCOMM Comput. Commun. Rev.*, vol. 41, no. 1, pp. 53–53, 2011.

[22] A. E. Kosba, A. Saeed, and M. Youssef, "Rasid: A robust WLAN device-free passive motion detection system," in *Proc. IEEE Int. Conf. Pervasive Comput. Commun. (PerCom).*, 2012, pp. 180–189.

[23] K. Qian, C. Wu, Z. Yang, Y. Liu, and Z. Zhou, "Passive detection of moving targets with dynamic speed using PHY layer information," in *Proc. 20th IEEE Int. Conf. Parallel Distrib. Syst.*, 2015, pp. 1–8.

[24] G. Wang, Y. Zou, Z. Zhou, K. Wu, and L. M. Ni, "We can hear you with wi-fi!" in *Proc. 20th Annu. Int. Conf. Mobile Comput. Netw.*, 2014, pp. 593–604.

[25] Q. Pu, S. Gupta, S. Gollakota, and S. Patel, "Whole-home gesture recognition using wireless signals," in *Proc. 19th Annu. Int. Conf. Mobile Comput. Netw.*, 2013, pp. 27–38.

[26] P. Melgarejo, X. Zhang, P. Ramanathan, and D. Chu, "Leveraging directional antenna capabilities for fine-grained gesture recognition," in *Proc. ACM Int. Joint Conf. Pervasive Ubiquitous Comput.*, 2014, pp. 541–551.

[27] X. Liu, J. Cao, S. Tang, and J. Wen, "Wi-sleep: Contactless sleep monitoring via wifi signals," in *Proc. IEEE Real-Time Syst. Symp.*, 2014, pp. 346–355.

[28] J. Liu, Y. Wang, Y. Chen, J. Yang, X. Chen, and J. Cheng, "Tracking vital signs during sleep leveraging off-the-shelf wifi," in *Proc. 16th ACM Int. Symp. Mobile Ad Hoc Netw. Comput.*, 2015, pp. 267–276.

[29] C. Han, K. Wu, Y. Wang, and L. M. Ni, "Wifall: Device-free fall detection by wireless networks," in *Proc. IEEE INFOCOM*, 2014, pp. 271–279.

[30] Y. Wang, J. Liu, Y. Chen, M. Gruteser, J. Yang, and H. Liu, "E-eyes: Device-free location-oriented activity identification using fine-grained wifi signatures," in *Proc. 20th Annu. Int. Conf. Mobile Comput. Netw.*, 2014, pp. 617–628.

[31] D. Zhang, H. Wang, Y. Wang, and J. Ma, "Anti-fall: A non-intrusive and real-time fall detector leveraging CSI from commodity WiFi devices," in *Proc. 13th Int. Conf. Inclusive Smart Cities e-Health*, 2015, pp. 181–193.

[32] P. Bahl and V. N. Padmanabhan, "Radar: An in-building RF-based user location and tracking system," in *Proc. INFOCOM 19th Annu. Joint Conf. IEEE Comput. Commun. Societies.*, 2000, pp. 775–784.

[33] B. Kellogg, V. Talla, and S. Gollakota, "Bringing gesture recognition to all devices," in *Proc. 11th USENIX Conf. Netw. Syst. Des. Implementation*, 2014, pp. 303–316.

[34] W. Xi, J. Zhao, X.-Y. Li, K. Zhao, S. Tang, X. Liu, and Z. Jiang, "Electronic frog eye: Counting crowd using WiFi," in *Proc. IEEE INFOCOM*, 2014, pp. 361–369.

[35] W. Liu, X. Gao, L. Wang, and D. Wang, "BFP: Behavior-free passive motion detection using PHY information," *Wireless Personal Commun.*, vol. 83, no. 2, pp. 1–21, 2015.

[36] C. Wu, Z. Yang, Z. Zhou, X. Liu, Y. Liu, and J. Cao, "Non-invasive detection of moving and stationary human with wifi,' *IEEE J. Selected Areas Commun.*, vol. 33, no. 11, pp. 2329–2342, 2015.

[37] S. Sigg, M. Scholz, S. Shi, Y. Ji, and M. Beigl, "Rf-sensing of activities from non-cooperative subjects in device-free recognition systems using ambient and local signals," *IEEE Trans. Mobile Comput.*, vol. 13, no. 4, pp. 907–920, Apr. 2014.

[38] J. Shea. (2005). An investigation of falls in the elderly [Online]. Available: http://www.signalquest.com/master

[39] D. Tse and P. Viswanath, *Fundamentals of Wireless Communication*. Cambridge, U.K.: Cambridge Univ. press, 2005.

[40] S. Sen, B. Radunovic, R. R. Choudhury, and T. Minka, "You are facing the Mona Lisa: Spot localization using PHY layer information," in *Proc. 10th Int. Conf. Mobile Systems, Appl., Serv.*, 2012, pp. 183–196.

[41] J. Gjengset, J. Xiong, G. McPhillips, and K. Jamieson, "Phaser: Enabling phased array signal processing on commodity wifi access points," in *Proc. 20th Annu. Int. Conf. Mobile Comput. Netw.*, 2014, pp. 153–164.

[42] C. Wu, Z. Yang, Z. Zhou, K. Qian, Y. Liu, and M. Liu, "Phaseu: Real-time los identification with WiFi," in *Proc. IEEE 33rd Annu. Int. Conf. Comput. Commun.*, 2015, pp. 2688–2696.

[43] R. Nandakumar, B. Kellogg, and S. Gollakota, "Wi-fi gesture recognition on existing devices," *arXiv preprint arXiv:1411.5394*, 2014.

[44] C. W. Han, S. J. Kang, and N. S. Kim, "Implementation of HMM-based human activity recognition using single triaxial accelerometer," *IEICE Trans. Fundam. Electron., Commun. Comput. Sci.*, vol. 93, no. 7, pp. 1379–1383, Jul. 2010.

[45] H. Kerdegari, K. Samsudin, A. R. Ramli, and S. Mokaram, "Evaluation of fall detection classification approaches," in *Proc. 4th Int. Conf. Intell. Adv. Syst.*, 2012, pp. 131–136.
[46] C. S. Hemalatha and V. Vaidehi, "Frequent bit pattern mining over tri-axial accelerometer data streams for recognizing human activities and detecting fall," *Procedia Comput. Sci.*, vol. 19, pp. 56–63, 2013.
[47] B. Schölkopf, A. J. Smola, R. C. Williamson, and P. L. Bartlett, "New support vector algorithms," *Neural Comput.*, vol. 12, no. 5, pp. 1207–1245, 2000.
[48] C.-C. Chang and C.-J. Lin, "Libsvm: A library for support vector machines," *ACM Trans. Intell. Syst. Technol.*, vol. 2, no. 3, p. 27, 2011.

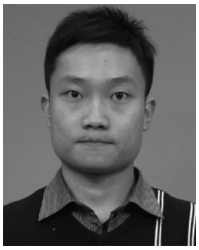

Hao Wang received the MS degree in software engineering from the School of Software and Microelectronics, Peking University, in 2013. He is currently working toward the PhD degree in computer science with the School of Electronics Engineering and Computer Science, Peking University. His research interests include mobile crowdsensing and ubiquitous computing. He is a student member of the IEEE.

Daqing Zhang received the PhD degree from the University of Rome La Sapienza in 1996. He is a chair professor in the School of EECS, Peking University, China. He has published more than 200 technical papers in leading conferences and journals. He served as the general or program chair for more than 10 international conferences, giving keynote talks at more than 16 international conferences. He is the associate editor for the *ACM Transactions on Intelligent Systems and Technology*, *IEEE Transactions on Big Data*, etc. He is the winner of the 10-years CoMoRea Impact Paper Award at the IEEE PerCom 2013, the Honorable Mention Award at the ACM UbiComp 2015, the Best Paper Award at the IEEE UIC 2015 and 2012, and the Best Paper Runner Up Award at Mobiquitous 2011. His research interests include context-aware computing, urban computing, mobile computing, big data analytics, pervasive elderly care, etc. He is a member of the IEEE.

Yasha Wang received the PhD degree in the Northeastern University, Shenyang, China, in 2003. He is currently a professor and associate director of the National Research & Engineering Center of Software Engineering, Peking University, China. He has published more than 50 papers in prestigious conferences and journals, such as ICWS, UbiComp, ICSP, etc. As a technical leader and manager, he has accomplished several key national projects on software engineering and smart cities. Cooperating with major smart-city solution providing companies, his research work has been adopted in more than 20 cities in China. His research interest includes urban data analytics, ubiquitous computing, software reuse, and online software development environment. He is a member of the IEEE.

Junyi Ma received the BE degree in network engineering from the School of Computer Science, Beijing University of Posts and Telecommunications, Beijing, China, in 2015. He is currently working toward the PhD degree in computer science in the School of Electronics Engineering and Computer Science, Peking University. His research interests include ubiquitous computing and mobile computing.

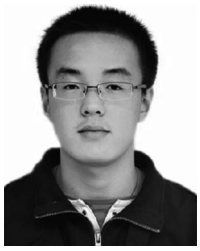

Yuxiang Wang is a senior at Peking University, studying computer science and technology. He is going to work toward the master's degree in the School of Electronics Engineering and Computer Science, Peking University. His main research interest is ubiquitous computing.

Shengjie Li received the BE degree in software engineering from Jilin University, Changchun, China, in 2015. She is currently working toward the PhD degree in computer science in the School of Electronics Engineering and Computer Science, Peking University. Her research interests include mobile crowd-sensing and ubiquitous computing.